

He, Ne and Ar composition of the European lithospheric mantle

Cécile Gautheron*, Manuel Moreira, Claude Allègre

*Laboratoire de Géochimie et Cosmochimie (UMR 7579 CNRS), IPGP, Université Denis Diderot (Paris 7),
4 place Jussieu 75252 Paris cedex 05, France*

Received 15 August 2003; received in revised form 20 December 2004; accepted 20 December 2004

Abstract

Rare gases have been measured in ultramafic xenoliths from European volcanic provinces, Dreiser Weiher (Germany), Massif Central (France) and Kapfenstein (Austria), to characterize the rare gas signature of a proterozoic subcontinental lithospheric mantle. The helium isotopic results, obtained by crushing of olivines, show values similar to the worldwide olivine xenocrysts and phenocrysts, with a very homogeneous, radiogenic helium isotopic ratio compared to that of the MORB source: $^4\text{He}/^3\text{He}=115,000\pm 7600$ ($R/Ra=6.32\pm 0.39Ra$ being the $^3\text{He}/^4\text{He}$ atmospheric ratio) compared to $\sim 90,000$ ($R/Ra=8$) for MORB, for a large range of ^4He concentration: 2×10^{-10} to 6×10^{-8} ccSTP/g. Neon and argon isotopic ratios show an important air component and nevertheless a mantle component, similar to MORB. The maximum $^{20}\text{Ne}/^{22}\text{Ne}$ and $^{40}\text{Ar}/^{36}\text{Ar}$ isotopic ratios measured in olivines are 10.65 and 6574, respectively. Elemental $^3\text{He}/^{36}\text{Ar}$ ratios appear strongly fractionated, suggesting helium diffusive loss from fluid inclusions to mineral matrix. The helium, neon and argon isotopic ratios argue against a lower mantle-derived plume responsible for the European Cenozoic volcanism, which is rather due to crustal extension and melting of the lithospheric mantle. Another possibility is that a mantle plume presently lies under the lithosphere, having triggered secondary plumes of lithospheric material from the lithosphere–asthenosphere boundary. To explain the homogenous helium isotopic signature of the European subcontinental lithospheric mantle, we discuss two possible models where asthenospheric helium invades the lithosphere: recent, local metasomatism and global, continuous metasomatism in steady state for helium. In the latter model, the derived ^4He flux is consistent with helium fluxes estimated for large areas such as the Pannonian basin and the Eger rift. The atmospheric component seen in Ne and Ar data is likely due to important air contamination of the xenoliths close to the surface, but may partly be possible evidence for subduction of atmospheric rare gases. Therefore, it is not meaningful to apply the steady state model to Ne and Ar.

© 2005 Elsevier B.V. All rights reserved.

Keywords: Rare gases; Helium flux; Mantle xenoliths; Subcontinental mantle; Europe

1. Introduction

The subcontinental lithospheric mantle (SCLM) is a peculiar Earth reservoir in terms of mantle convection and geochemistry. It is isolated from the

* Corresponding author. Now at Laboratoire IDES (UMR 8148 CNRS), Université Paris XI, 91405 Orsay, France.

E-mail address: gautheron@geol.u-psud.fr (C. Gautheron).

convective mantle and therefore should have a specific chemical signature compared to the convective mantle. Trace element and Pb–Sr–Nd isotopic studies have shown that the SCLM is similar to a normal oceanic mantle to which fluids coming from the asthenosphere or slab dehydration during past subductions were added. These percolating fluids and/or melts are enriched in incompatible elements, as illustrated in kimberlites, ultramafic xenoliths and alkali basalts (Hawkesworth et al., 1984; Porcelli et al., 1986; Stosch et al., 1986; Menzies et al., 1987; Kempton et al., 1988). This process enriches the supposed depleted lithospheric mantle and therefore, the trace elements and isotope budget is not well constrained but certainly not depleted. Due to the low rare gas content of the continental area xenoliths, previous studies were focused on helium, showing that the helium isotopic ratio is more radiogenic than that of the MORB source (Porcelli et al., 1986, 1987, 1992; Dunaï and Baur, 1995; Reid and Graham, 1996; Matsumoto et al., 1998, 2000; Ackert et al., 1999; Barfod et al., 1999; Dunaï and Porcelli, 2002; Gautheron and Moreira, 2002). The origin of this radiogenic helium is still debated. It has been attributed to a mantle plume having low $^3\text{He}/^4\text{He}$ ratio, to addition of sediments to a MORB source mantle (Hanyu and

Kaneoka, 1997) or to a feature of the subcontinental mantle itself. The neon and argon isotopic signature of the SCLM is even less constrained than helium and shows only small anomalies compared to air (Matsumoto et al., 1998, 2000; Barfod et al., 1999). The strong atmospheric component can be explained by atmospheric contamination or by a recycled atmospheric component in the lithospheric mantle. In addition, Matsumoto et al. (2001) have shown the possibility of atmospheric rare gas recycling to the lithospheric mantle and the SCLM is a possible reservoir of atmospheric rare gases due to past subduction. If storage of atmospheric rare gases in the lithospheric mantle is a general phenomenon, this can be very important for rare gas budgets because the SCLM can be delaminated and recycled into the convecting mantle (Seber et al., 1996).

In order to address these issues, we have performed new crushing analyses of He, Ne and Ar in olivines from lherzolites and harzburgites sampled in three European volcanic provinces (Massif Central, Eifel, Kapfenstein). Our new He, Ne and Ar results suggest that the subcontinental mantle contains fluids similar in isotopic compositions to the MORB source mantle plus a radiogenic/nucleogenic component reflecting higher U+Th/He and K/Ar ratios of either the fluids or the subcontinental mantle itself. Additionally, a large

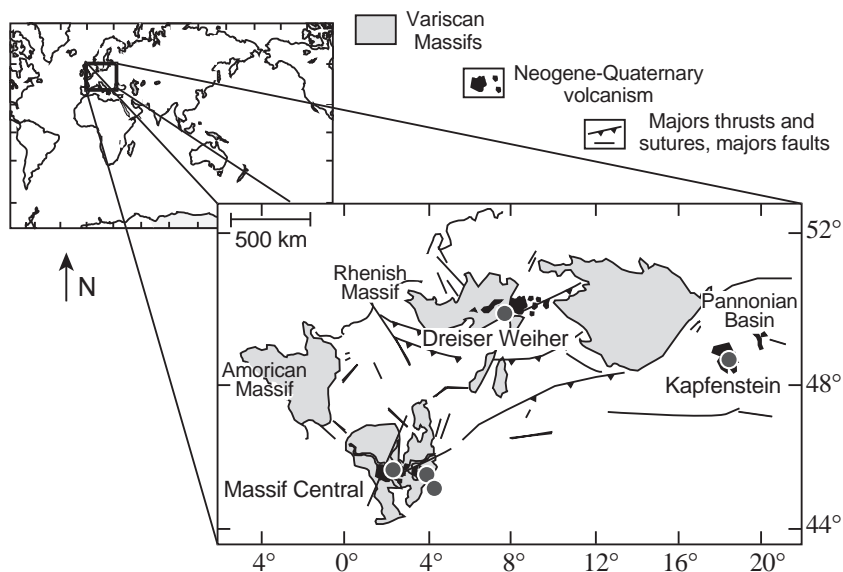


Fig. 1. Location of the European xenoliths studied (gray circles).

Table 1
Sample locations of the xenoliths from the three studied volcanic provinces, France, Germany and Austria

Sample	Regions	Locality
MC98-01	Chaîne de la Sioule	Sauterre
MC98-03	Chaîne des puys	Rochemonteix
MC98-05	Vivarais	Saint-Pierre
MC98-06	Vivarais	Burzet
MC98-07	Devez	Mont Briançon
MC98-08	Devès	St. Arcons
MC98-09	Devès	Mont Coupet
MC95-44	Chaîne de la Sioule	Beaunit
DWC1	Eifel	Dreiser Weiher
PFS31	Eifel	Dreiser Weiher
PFS77	Eifel	Dreiser Weiher
Eifel 228	Eifel	Dreiser Weiher
EK2	Kempenich	Dreiser Weiher
GM3	Geeser Maar	Geeser Maar
KA200	Pannonian Basin	Kapfenstein
KA7	Pannonian Basin	Kapfenstein

air contamination affects the samples, probably during their emplacement.

2. Samples and analytical procedure

The ultramafic xenoliths from Europe were sampled in Dreiser Weiher (Germany), Massif Central (France) and Kapfenstein (Austria) (Fig. 1). Sample locations are reported in Table 1. The peridotites from Dreiser Weiher were collected at Dreiser Weiher and

Kempenich Volcanoes (Rhenish Massif). The two spinel lherzolites from the Pannonian basin (central Europe) were sampled in Kapfenstein (Dunai and Baur, 1995). Some of the samples were already analyzed for He, Ne and Ar using melting by Dunai and Baur (1995), where neon was analyzed but with very large uncertainties that do not allow any clear conclusion. Xenoliths from Massif Central (Central France) were sampled in several volcanic provinces: Chaîne de la Sioule, Chaîne des puys, Cantal, Vivarais and Devès. The carrier basalts are principally alkali basalts and come from melting of an enriched mantle (Wilson and Downes, 1991). Major and trace element compositions show no pristine xenoliths. They are in majority coarse spinel harzburgites and spinel lherzolites. Hydrous and anhydrous peridotites are present and are characterized by amphibole or phlogopite occurrence and absence, respectively (Stosch, 1987). The Cenozoic volcanism in this area can be explained by extensive rifting or by the presence of a mantle plume under the crust (Hoernle et al., 1995; Goes et al., 1999; Wedepohl and Baumann, 1999). Furthermore, before this recent volcanism, the Hercynian orogenesis may have influenced the mantle by several stages of metasomatism between 360 and 260 Ma, as illustrated by vestiges of a back-arc basin in Marvejols, France (Leyreloup, 1992). The trace elements and Sr, Nd, Pb, O isotopes were then affected in the Massif Central, Dreiser Weiher and Kapfenstein mantles (Stosch and Seck, 1980; Chauvel and Jahn,

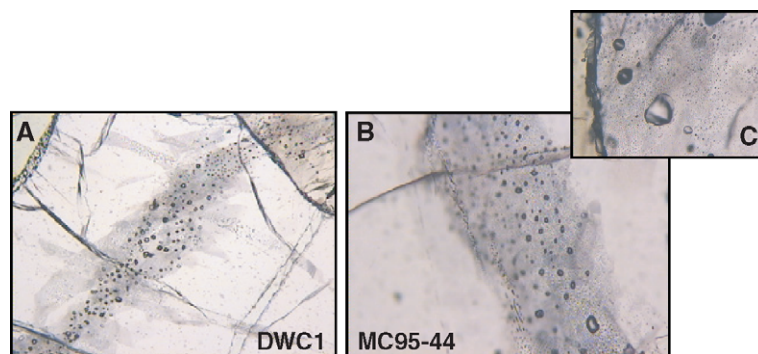


Photo 1. Photographs of thin sections in mantle xenoliths: (A) DWC1 ($\times 4$), (B) MC95-44 ($\times 4$) and (C) inclusions of MC95-44 ($\times 500$). The size of the inclusions on photo C ranges between 15 and 30 μm . In photo A, a row of fluids inclusions can be seen crossing the boundary between olivine and pyroxene (mineral on top right). The same kind of fluids inclusions is visible in Photo B. Photo C is a close-up of Photo B showing several CO_2 -rich fluid inclusions (the CO_2 inclusion is clearly visible in the largest one) characterized by a homogenization temperature of 25 $^\circ\text{C}$.

1983; Seck and Wedepohl, 1983; Stosch and Lugmair, 1986; Wörner et al., 1986; Kempton et al., 1988; Rosenbaum and Wilson, 1997).

Only olivines were analyzed in this study, and only by crushing. This is to avoid secondary radiogenic–nucleogenic production of He, Ne and Ar (olivine is a U–Th–K free mineral) or cosmogenic He and Ne. Samples were cleaned with distilled water, ethanol and acetone in an ultrasonic bath. He, Ne and Ar were analyzed, using the glass mass spectrometers ARE-SIBO I and II in Paris. Crushing or step crushing was applied for samples with weights between 0.45 and 1.21 g. DWC1 was leached with 7N HF three times during 30 minutes and extensively cleaned with distilled water, ethanol and acetone. The blanks were $\sim 4 \times 10^{-9}$ for ^4He , $\sim 4 \times 10^{-13}$ for ^{22}Ne and $\sim 1.5 \times 10^{-12}$ for ^{36}Ar , all in ccSTP, with atmospheric isotopic compositions within uncertainties. Some helium measurements on olivines (0.2–0.3 g) were also performed at the Woods Hole Oceanographic Institution (WHOI) with a ^4He blank of $\sim 5 \times 10^{-11}$ ccSTP. Additionally, neon content and isotopic ratios were measured on a duplicate of sample DWC1 at Woods Hole Oceanographic Institution with a ^{22}Ne blank of $\sim 10^{-13}$ ccSTP (Moreira et al., 2001).

3. Fluids inclusions

A characterization of fluid inclusion morphology was performed. Several fluid and melt inclusion generations were observed in the samples. For example, MC95-44 and DWCI show the same kind of inclusions but in different proportions (Photo 1). MC95-44 possesses three generations of inclusions. “Primary” inclusions never crosscut the grain boundaries. They are bi-phased, i.e. they have both a solid silicate phase, consisting of glass and crystals, and a fluid phase with vapor and liquid. This kind of inclusion was described by Andersen and Neuman (2001). Secondary inclusions are CO_2 -rich, and are characterized by a homogenization temperature near 25 °C. Both generations of inclusions cross cut each other. The third generation is composed of fluid inclusions that cross cut with each other, making identification of content difficult. Nevertheless, one can note in the pyroxenes H_2O -rich fluid exsolutions due to xenolith decompression. DWC1 possesses a

similar quantity of primary inclusions, but less CO_2 -rich inclusions than MC95-44.

4. Results

Helium results measured at WHOI are reported in Table 2 and those obtained in Paris in Table 3. Helium concentrations and isotopic compositions were obtained by crushing that allows the analysis of the helium trapped in fluid inclusions rather than that located in matrix. The rare gases in ultramafic xenoliths are in CO_2 inclusions (Porcelli et al., 1986). Because of lower helium blanks, we use only the WHOI data reported in Table 2. European ultramafic xenoliths are characterized by helium isotopic ratios ranging from 84,020 to 200,000 ($\text{R}/\text{Ra}=3.6\text{--}8.6$)

Table 2
Helium content and isotopic ratios of xenoliths (olivines) from Europe

Samples	^4He ccSTP/g	R/Ra ($\pm 1\sigma$)	$^4\text{He}/^3\text{He}$ ($\pm 1\sigma$)
<i>Dreiser Weiher</i>			
DWC1-a	2.0×10^{-8}	6.15 ± 0.1	$117,500 \pm 1900$
DWC1-a recrush	6.7×10^{-9}	6.15 ± 0.14	$117,500 \pm 2670$
DWC1-a Total	2.6×10^{-8}	6.15 ± 0.11	$117,500 \pm 2140$
PFS31-a	2.5×10^{-9}	6.39 ± 0.15	$113,100 \pm 2700$
PFS77-a	5.6×10^{-8}	6.73 ± 0.11	$107,400 \pm 1800$
GM3-b	5.6×10^{-9}	5.52 ± 0.09	$131,000 \pm 2100$
EK2-b	1.3×10^{-9}	6.31 ± 0.15	$114,500 \pm 2700$
<i>Kapfenstein</i>			
KA7-b	2.2×10^{-10}	8.6 ± 0.8	$84,020 \pm 7800$
KA200-a	2.5×10^{-9}	6.65 ± 0.14	$108,650 \pm 2300$
KA200-a recrush	7.8×10^{-10}	6.44 ± 0.16	$112,200 \pm 2800$
KA200-a Total	3.3×10^{-9}	6.6 ± 0.12	$109,480 \pm 1990$
<i>Massif Central</i>			
MC98-01-b	2.3×10^{-10}	3.62 ± 0.95	$200,000 \pm 52,400$
MC98-03-b	7.4×10^{-10}	5.43 ± 0.22	$133,100 \pm 5400$
MC98-05	7.2×10^{-10}	6.91 ± 0.3	$104,570 \pm 4800$
MC98-06-b	1.8×10^{-9}	6.21 ± 0.2	$116,540 \pm 3800$
MC98-07-a	6.9×10^{-10}	6.66 ± 0.6	$108,500 \pm 9780$
MC98-07-a recrush	1.9×10^{-10}	6.20 ± 0.93	$116,500 \pm 17,500$
MC98-07-a Total	8.8×10^{-10}	6.57 ± 0.67	$109,980 \pm 11,300$
MC98-08-b	3.9×10^{-10}	6.56 ± 0.43	$110,100 \pm 7200$
MC98-09-a	3.7×10^{-10}	6.62 ± 0.88	$109,150 \pm 14,500$
MC95-44	9.0×10^{-9}	6.68 ± 0.06	$108,170 \pm 1000$

Analyses were performed at Woods Hole Oceanographic Institution by Manuel Moreira and Joshua Curtice in the Isotope Facility lab directed by Mark Kurz. Experimental procedure is detailed in Moreira et al. (2001).

Table 3

Helium, neon and argon concentrations (in ccSTP/g) and isotopic ratios measured in xenoliths from Europe

	Weight (g)	^4He ($\times 10^{-8}$)	$^4\text{He}/^3\text{He}$	^{22}Ne ($\times 10^{-12}$)	$^{20}\text{Ne}/^{22}\text{Ne}$	$^{21}\text{Ne}/^{22}\text{Ne}$	^{36}Ar ($\times 10^{-12}$)	$^{40}\text{Ar}/^{36}\text{Ar}$
<i>Dreiser Weiher</i>								
DWC1-WHOI	0.3240	2.63±0.01	109,642±1497	2.58±0.01	10.31±0.10	0.0351±0.0013	n.m.	n.m.
DWC1-a	0.6592	1.30±0.02	124,972±57,500	2.14±0.24	10.45±0.25	0.0371±0.0039	37.80±3.87	1701±284
DWC1-b	1.2080	3.77±0.17	115,155±9000	1.37±0.07	10.44±0.18	0.0336±0.0019	32.51±0.27	4300±91
DWC1-c step1	1.2080	2.61±0.11	109,016±14,200	0.73±0.05	10.27±0.20	0.0384±0.0043	15.12±0.21	6574±146
DWC1-c step2	1.2080	1.55±0.07	114,323±14,000	0.76±0.06	10.07±0.17	0.0305±0.0026	14.22±0.08	3586±75
Total	1.2080	4.16±0.10	110,994±14,100	1.49±0.06	10.17±0.19	0.0344±0.0034	29.34±0.15	5126±112
DWC1-d	1.0968	7.92±0.31	108,842±7000	1.72±0.05	10.65±0.14	0.0414±0.0027	37.09±0.18	4776±98
EK2-a	0.6641	0.10±0.01	b.l.	5.81±0.59	10.04±0.12	0.0280±0.0010	24.37±2.52	314±53
EK2-b	1.2038	0.25±0.01	b.l.	0.97±0.06	10.03±0.18	0.0273±0.0024	33.25±0.17	330±7
PFS31-a	0.6796	4.00±0.06	b.l.	6.95±0.73	n.d.	n.d.	11.48±1.22	484±82
PFS31-b	1.2005	0.39±0.02	b.l.	5.06±0.24	9.85±0.08	0.0292±0.0011	46.07±0.16	353±7
GM3	1.2006	1.61±0.07	178,666±26,000	9.79±0.12	9.70±0.07	0.2946±0.0150	313.22±0.54	378±8
Eifel228	0.8964	2.46±0.08	105,180±13,600	19.94±0.19	10.09±0.08	0.0296±0.0005	69.06±0.2	1201±24
PFS77	0.5600	8.69±0.18	106,201±6100	2.40±0.11	10.28±0.21	0.0348±0.0023	45.55±0.15	2252±47
<i>Kapfenstein</i>								
KA7	0.6500	b.l.	b.l.	0.08±0.06	n.d.	n.d.	5.10±0.52	340±60
KA200	0.6791	0.13±0.01	b.l.	0.34±0.19	n.d.	n.d.	6.37±0.67	528±90
<i>Massif Central</i>								
MC95-44	1.2050	1.86±0.08	107,845±13,400	20.73±0.13	9.89±0.05	0.0296±0.0004	393.5±0.48	370±7
MC98-05	1.2041	0.40±0.01	157,216±78,000	0.50±0.01	10.02±0.1	0.0294±0.0013	8.54±0.02	469±13
MC98-06	1.2020	0.03±0.01	b.l.	0.20±0.01	9.84±0.13	0.0270±0.0015	1.24±0.01	1141±33
MC98-09	1.2020	0.08±0.01	b.l.	5.38±0.09	9.78±0.08	0.0287±0.0008	72.49±0.20	311±8

Because the extraction method was crushing, the concentration values are minimum. DWC1 shows well a mantle component, and for this reason it was analyzed four times (2 total crushing (a and b), one step-crushing (c step1, c step2 and total), and after a leach with H.F. (d)). b.l. means blank level, n.m. not measured and n.d. not determined. Atmospheric isotopic ratios are from Ozima and Podosek (1983).

(Table 2). The mean ratio is $^4\text{He}/^3\text{He}=118,000$ ($R=6.33\text{Ra}$), more radiogenic than the mean MORB ratio ($^4\text{He}/^3\text{He}=90,000\pm 10,000$; $R/\text{Ra}=8\pm 1$; Allègre et al., 1995). Except for two samples, this helium signature is constant over a large range of helium contents (Fig. 2). The helium isotopic ratio is comparable to the results obtained by melting ($^4\text{He}/^3\text{He}=116,350\pm 45,340$ or $R=(6.21\pm 2.42)\text{Ra}$; Dunai and Baur, 1995) for European xenoliths. It is also comparable to gas collected in lakes: $^4\text{He}/^3\text{He}=134,800\pm 500$ or $R/\text{Ra}=5.36\pm 0.02$ for the Laacher See (Germany) (Aeschbach-Hertig et al., 1996) and $^4\text{He}/^3\text{He}=109,980\pm 170$ or $R/\text{Ra}=6.57\pm 0.01$ for the lac Pavin (France) (Aeschbach-Hertig et al., 1999). It is remarkable that the helium isotopic signature of the European province is so homogeneous for a very extended zone and for different kinds of samples (xenoliths, water). The range of ^4He concentrations is large and varies from 2×10^{-10} (MC98-01-b) to 6×10^{-8} ccSTP/g (PFS77-

a). It is similar to published helium contents for xenoliths and phenocrysts from Australia and the Cameroon line (Matsumoto et al., 1998, 2000; Barfod et al., 1999).

Samples MC98-01 and KA7 have significantly different helium isotopic ratios compared to the mean ratio ($^4\text{He}/^3\text{He}=200,000$ and $84,020$, respectively). Secondary processes such as in-situ radiogenic and cosmogenic production could explain these ratios. Sample MC98-01 has a very radiogenic ratio ($^4\text{He}/^3\text{He}=200,000\pm 52,400$ or $R/\text{Ra}=3.6\pm 1.0$) that may derive from U and Th decay after eruption of the host lava. This effect is very significant for such a low concentration ($^4\text{He}=2.3\times 10^{-10}$ ccSTP/g). Similarly, sample KA7 ratio ($^4\text{He}/^3\text{He}=84,020\pm 7800$ or $R/\text{Ra}=8.6\pm 0.8$, $^4\text{He}=2.2\times 10^{-10}$ ccSTP/g) could be explained by the production of cosmogenic ^3He (Kurz, 1986). Radiogenic or cosmogenic helium can also be released during crushing in small quantities (by diffusion) from the matrix. The effect becomes

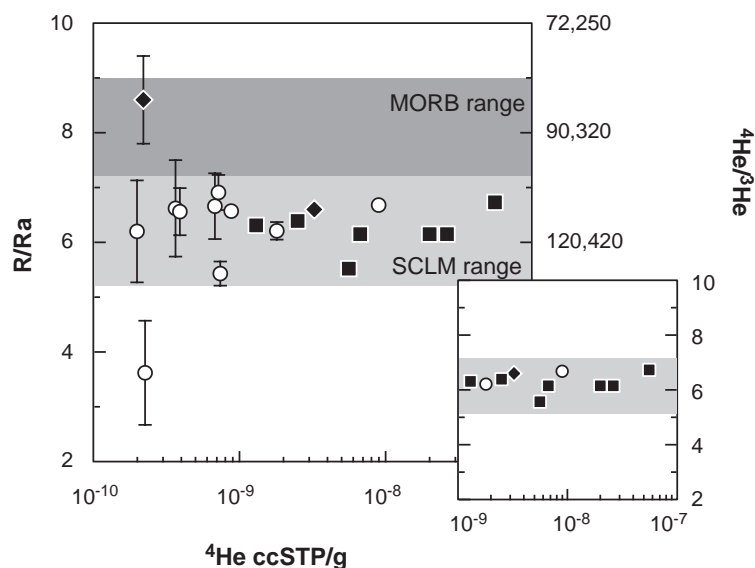


Fig. 2. Helium isotopic ratio ($^4\text{He}/^3\text{He}$ and R/Ra) versus ^4He concentration in ccSTP/g. The typical MORB and SCLM range are reported (Allègre et al., 1995; Gautheron and Moreira, 2002). In this figure, the three different volcanic regions are distinguished: black square: Dreiser Weiher (Germany), black diamonds: Kapfenstein (Austria) and white circle: Massif Central (France). Helium isotopic ratios for European xenoliths are very homogenous and are more radiogenic than MORB. In the insert, only samples with ^4He concentration higher than 10^{-9} ccSTP/g are kept (cut-off value); the mean isotopic ratio becomes $R/Ra=6.32\pm 0.39$ or $^4\text{He}/^3\text{He}=115,000\pm 7600$.

significant for low He contents. In order to remove such secondary processes (radiogenic and cosmogenic effects), an arbitrary cut-off value for the ^4He concentration (10^{-9} ccSTP/g) is used. Radiogenic and cosmogenic helium are negligible for concentrations higher than 10^{-9} ccSTP/g as illustrated in Fig. 2. Such a notion of cut-off value was already used by Dunai and Baur (1995), who took a value of 10^{-7} ccSTP/g for the ^4He (they melted the samples and therefore the effect of the helium located in the matrix is more important). With the introduction of this cut-off value, the standard deviation of the helium isotopic ratios becomes smaller $^4\text{He}/^3\text{He}=115,000\pm 7600$ or $R/Ra=6.32\pm 0.39$ (Fig. 2).

To constrain the helium content located in the crystal matrix, 3 powders coming from previous crushing (PFS77, MC98-06 and MC95-44) were melted. The results are given in Table 4. The isotopic ratios are similar in the inclusions and in the powders showing that cosmogenic or radiogenic helium is negligible for most of the samples (PFS77-a: $^4\text{He}/^3\text{He}_{\text{crushed}}=106,300\pm 1,500$ or $R/Ra_{\text{crushed}}=6.8\pm 0.1$ and $^4\text{He}/^3\text{He}_{\text{powder}}=107,850\pm 1600$ or $R/Ra_{\text{powder}}=6.7\pm 0.1$). The concentration in the powder, obtained

by melting, is usually higher by a factor ~ 2 than the content obtained by crushing. This may reflect incomplete crushing of the sample.

Neon concentrations and isotopic ratios are reported in Table 3. ^{22}Ne concentrations vary from 8×10^{-14} to 2×10^{-10} ccSTP/g, similar to published data on similar samples (Matsumoto et al., 1998, 2000). The samples present isotopic anomalies compared to the atmospheric ratios with a maximum of 10.65 for the $^{20}\text{Ne}/^{22}\text{Ne}$ ratio and fall close to the MORB line (Sarda et al., 1988) in the $^{20}\text{Ne}/^{22}\text{Ne}$ – $^{21}\text{Ne}/^{22}\text{Ne}$ diagram (Fig. 3). The samples show a strong air-component, similarly to other SCLM xenoliths and lakes (Aeschbach-Hertig et al., 1996; Matsumoto et al., 1998, 2000; Barfod et al., 1999), with a maximum $^{20}\text{Ne}/^{22}\text{Ne}$ isotopic ratio measured in xenoliths (by

Table 4

Helium content (in ccSTP/g) and isotopic ratio in powder samples from previous analyses

Name	^4He melt	R/Ra melt	^4He crush	R/Ra crush
PFS77 ol	1.3×10^{-7}	6.8 ± 0.1	5.6×10^{-8}	6.7 ± 0.1
MC98-06 ol	3.3×10^{-9}	7.2 ± 0.2	1.8×10^{-9}	6.2 ± 0.2
MC95-44 ol	1.0×10^{-8}	6.9 ± 0.1	9.0×10^{-9}	6.7 ± 0.1

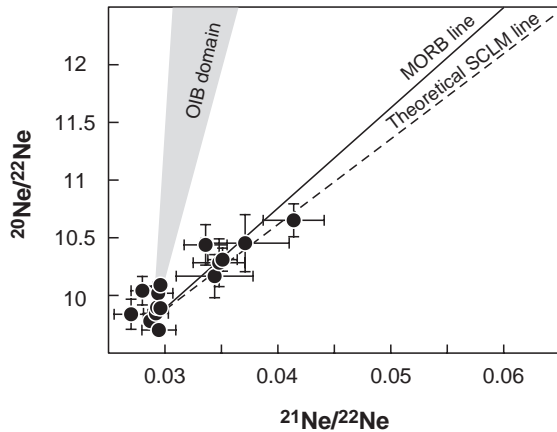


Fig. 3. Ne–Ne isotopic diagram. Reported for the comparison of the MORB line defined by Sarda et al. (1988) and the OIB domain (Staudacher et al., 1990; Honda et al., 1991; Hiyagon et al., 1992; Poreda and Farley, 1992; Dixon et al., 2000; Moreira et al., 2001). Data show mixing between a component similar to the MORB source and an air component. The line labeled SCLM is the theoretical line corresponding to a $^4\text{He}/^3\text{He}$ of 115,000, more radiogenic than the MORB value. This calculation assumes a closed system model for ^{21}Ne ingrowth and a $^{21}\text{Ne}/^4\text{He}$ production ratio of 4.5×10^{-8} .

crushing) of 11.9 ± 0.26 (Barfod et al., 1999). Fig. 3 shows a mixture between two components. One is a component with the air composition and the second a component similar to the MORB reservoir ($^{20}\text{Ne}/^{22}\text{Ne} > 11$ and $^{21}\text{Ne}/^{22}\text{Ne} > 0.05$). The variation of the

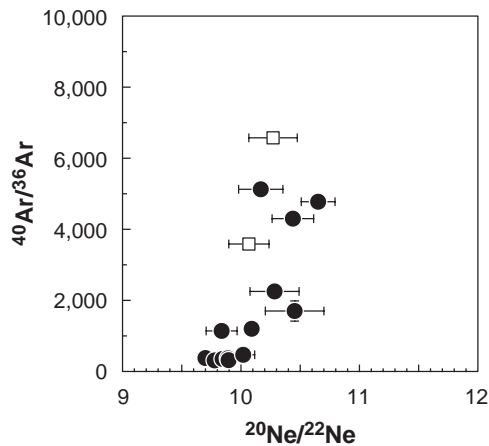


Fig. 4. Mark $^{40}\text{Ar}/^{36}\text{Ar}$ as a function of $^{20}\text{Ne}/^{22}\text{Ne}$. As in Fig. 3, a binary mixing for neon and argon between a source similar to the MORB mantle and an atmospheric component is observed. The black circles represent the totals and the empty squares the step-crushing analysis on DW1.

$^{21}\text{Ne}/^{22}\text{Ne}$ ratio reflects the production of ^{21}Ne by nuclear reactions in the mantle (Kyser and Rison, 1982). A discussion exists about the value of the $^{20}\text{Ne}/^{22}\text{Ne}$ isotopic ratio in the MORB source mantle, which could be 12.5 (Ne–B; Dixon et al., 2000; Trieloff et al., 2000) or 13.8 (Solar; Honda et al., 1991; Sarda et al., 2000). This debate has no effect on the following and, in this paper, we will use a $^{20}\text{Ne}/^{22}\text{Ne}$ of 13.8 for the calculations.

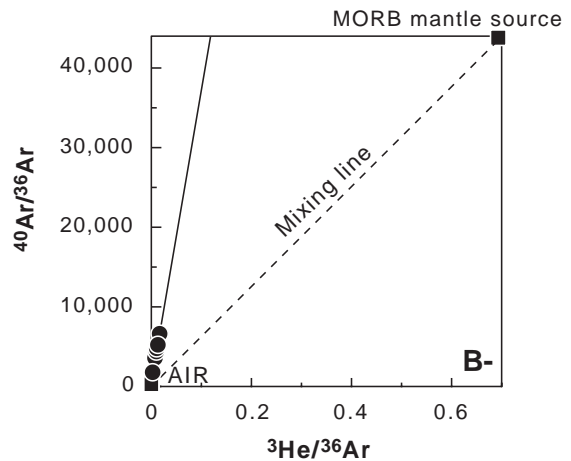
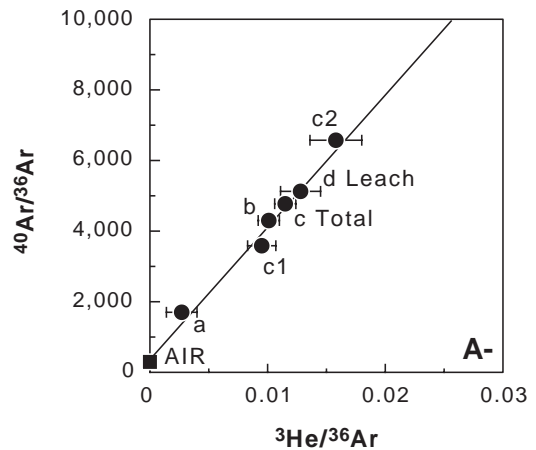


Fig. 5. (A) $^{40}\text{Ar}/^{36}\text{Ar}$ as a function of the elemental ratio $^3\text{He}/^{36}\text{Ar}$ for sample DW1. All the steps are represented. The line is a mixing line between atmosphere and a mantle component. (B) Extended version of (A). The dashed line shows what mixing between air and the MORB mantle source would look like. The plain line extends the DW1 linear correlation, showing that the $^3\text{He}/^{36}\text{Ar}$ of the lithospheric mantle component end-member would be about 0.11 for this sample.

Argon concentrations and the $^{40}\text{Ar}/^{36}\text{Ar}$ isotopic ratios are reported in Table 3. ^{36}Ar concentrations vary from 1×10^{-12} to 4×10^{-9} ccSTP/g, similar to previous studies (Kyser and Rison, 1982; Matsumoto et al., 1998, 2000). The $^{38}\text{Ar}/^{36}\text{Ar}$ isotopic ratios are indistinguishable from the atmospheric ratio ($^{38}\text{Ar}/^{36}\text{Ar}=0.1880$) and therefore are not reported in Table 3. The $^{40}\text{Ar}/^{36}\text{Ar}$ isotopic ratios range between atmospheric (295.5) and a radiogenic value of 6574 (DWC1c-2). The maximum argon isotopic ratio measured in continental area xenoliths by crushing is 9600 (Kyser and Rison, 1982). All these data indicate an important air-like component in the source of worldwide xenoliths. The origin of the high $^{40}\text{Ar}/^{36}\text{Ar}$ ratios compared to air can reflect either the production of ^{40}Ar by decay of ^{40}K or mixing between air and a mantle component ($^{40}\text{Ar}/^{36}\text{Ar}$ up to 44,000; Moreira et al., 1998). Olivine is a K-poor mineral (<25 ppm except for KA200 with a K content of 100 ± 7 ppm; Gautheron, unpublished data). Ar and Ne isotopic ratios are correlated, as illustrated on Fig. 4, indicating that the origin of the high $^{40}\text{Ar}/^{36}\text{Ar}$ has principally a mantle origin. Additionally, Fig. 5 shows the strong correlation between the $^{40}\text{Ar}/^{36}\text{Ar}$ and $^3\text{He}/^{36}\text{Ar}$ ratios, again representing a two component mixing.

5. Discussion

To explain the helium signature measured in European subcontinental mantle xenoliths, a plume source model for the European Cenozoic volcanism has been proposed by some authors (Hoernle et al., 1995; Goes et al., 1999; Wedepohl and Baumann, 1999). Our preferred model is that the peculiar helium signature is a feature of the subcontinental mantle with no involvement of a deep mantle plume. The possibility that the SCLM can be an important reservoir of atmospheric rare gases will also be discussed.

5.1. Origin of the helium signature

The helium isotopic ratios for European xenoliths center around a very uniform, but radiogenic value compared to MORB ($^4\text{He}/^3\text{He}=115,000$ or $R=6.32$ Ra). This observation is true for a large range of helium concentrations. Due to the very low helium

concentration in air, atmospheric contamination is negligible. Therefore, the helium isotopic ratio can represent either a source feature or post-eruptive radioactive decay of uranium and thorium.

5.1.1. Post-eruptive helium?

Crushing the samples permits extraction of the gas contained in CO_2 or H_2O inclusions, usually free of uranium and thorium. Moreover, we analyzed olivine, a mineral poor in uranium and thorium. This excludes a secondary origin for the radiogenic ratio as confirmed by the melting analyses of powder after crushing (Table 4). A secondary origin also fails to explain the homogeneity of the ratios, since it would imply that all the samples have the same $(\text{U}+\text{Th})/^3\text{He}$ contents and the same age of eruption. This is unlikely. Therefore, the helium isotopic ratios have to reflect the mantle signature. Two origins are then possible. One is a mantle plume, with an appropriate helium isotopic ratio. The helium signature could also be a feature of the subcontinental mantle.

5.1.2. Helium from a mantle plume?

A percolating primitive plume cannot explain the helium isotopic ratio of the European subcontinental lithospheric mantle. In contrast to the Deccan, Afar and Yellowstone volcanic areas, that present plateaus of flood basalts with a thickness of a few kilometers, the European volcanism is concentrated in extension zones with much smaller quantities of mafic rocks. Further, the Deccan, Afar and Yellowstone traps show high $^3\text{He}/^4\text{He}$ signatures, compatible with primitive mantle plumes (Basu et al., 1993; Marty, 1993; Dodson et al., 1997), while the helium ratio obtained for the European volcanism is similar to the MORB ratio, although it is slightly more radiogenic.

Some existing hotspots have a more radiogenic helium than MORB (e.g. Tubuai, St Helena, Canaries, Sao Miguel in the Azores) but are very small in volume compared to all hotspots (Graham et al., 1992; Hanyu and Kaneoka, 1997; Moreira et al., 1999). Some authors working on European xenoliths and lavas argue for the presence of a HIMU plume in the source (Dunai and Baur, 1995; Wilson and Downes, 1991). However, HIMU is associated with extreme signatures in lead or strontium isotopes, which is not the case of Massif Central or Dreiser Weiher. All the hotspots with Sr–Pb signatures similar to that of

Massif Central or Dreiser Weiher (i.e. moderate Sr and Pb ratios) show primitive helium ratios (Hart et al., 1992). For these reasons, other hypotheses are preferred.

Additionally, the helium isotopic ratio is very homogenous for a large range of helium contents and various locations through Europe. Most continental volcanic areas in the world show the same helium ratio. Therefore, the helium isotopic ratios of the xenoliths represent the lithospheric mantle signature rather than deep mantle helium with a low $^4\text{He}/^3\text{He}$ ratio. However, recent laboratory fluid experiments (Jurine et al., 2003) have shown that, when a plume arrives under the lithosphere, a secondary plume, starting at the lithosphere–asthenosphere boundary, can be produced within the lithosphere. This suggests that a deep mantle-derived plume may exist under the Massif Central or Eiffel, but the signature at the surface only reflects the SCLM.

5.1.3. Subcontinental lithospheric helium

The SCLM thus appears to have a MORB-like, slightly radiogenic helium isotopic signature. This can be explained (1) by addition, at subduction zones, of ^4He -rich fluids, and/or melt, to a lithosphere with MORB helium, or (2) by a closed system evolution starting with MORB helium, or else (3) by introduction of rare gas bearing fluids to the subcontinental reservoir from the asthenosphere, either recently, in preferential areas, or to the entire lithosphere along geological periods of time.

5.1.3.1. Fluids from subducting plate. Addition of fluids/melts rich in ^4He or with a high $\text{U}/^3\text{He}$ ratio can be caused by dehydration of a subducting plate (e.g. Yamamoto et al., 2004). Indeed, episodes of subduction are invoked in the European subcontinental lithosphere in order to explain the presence of eclogite (Leyreloup, 1992), the trace element signatures and the Sr–Nd systematics (Wilson and Downes, 1991). Dunaï and Baur explain the helium ratio by the presence of 1–2% of sediments in the European lithosphere corresponding to a subduction event (Dunaï and Baur, 1995). Such an introduction of fluids is a local phenomenon and the amount of introduced sediments can be very variable for different subduction zones (Tatsumi and Kogiso, 1997). The homogenization of the U and Th content in the

European SCLM is unlikely, like the constancy of the helium isotopic signature in this model. Indeed, very low $^3\text{He}/^4\text{He}$ ratios were reported for xenoliths from Eastern Russia, where subduction occurred during the Mesozoic (Yamamoto et al., 2004). However, we cannot totally reject this model, even if we don't think it can explain the homogenous signature of the subcontinental mantle worldwide: Europe, Australia, Western and Southwestern USA, Antarctic, Cameroon (Gautheron and Moreira, 2002; and reference therein).

5.1.3.2. Closed-system lithosphere. A closed-system model was proposed by Reid and Graham (1996) and Dodson et al. (1998). This model implies a $\text{U}/^4\text{He}$ ratio of 1000 to 2000 (U in ppm and ^4He in ccSTP/g). For a ^4He content of 10^{-6} ccSTP/g in the subcontinental mantle, the U concentration should thus be near 1–2 ppb. This concentration is too low compared to the uranium content of the MORB source (5–6 ppb) and is incompatible with the enriched signature of the subcontinental mantle. The case is worse if the subcontinental mantle has less than $1 \mu\text{ccSTP/g}$ ^4He . Knowledge of the helium content in the SCLM is delicate but the worldwide data indicate a ^4He of about 10^{-7} ccSTP/g (Gautheron and Moreira, 2002). Furthermore, a closed system model with 5–6 ppb U necessitates a helium content in the subcontinental mantle higher than $1 \mu\text{ccSTP/g}$ to explain the peculiar helium isotopic ratio of the European ultramafic xenoliths; otherwise the $^3\text{He}/^4\text{He}$ ratio becomes too low. No data indicate such a high helium content for the European SCLM (Tables 2 and 3 and Dunaï and Baur, 1995). Although this may be measured in the future for some samples, and the helium concentration in the SCLM is still an object of debate, present knowledge seems to invalidate the closed-system approach. Therefore, we prefer to explore another model.

5.1.3.3. Asthenosphere-derived fluids. A third model can be proposed where metasomatic fluids percolate from the asthenospheric mantle to the SCLM. This hypothesis was already mentioned in the literature to explain, for example, the re-enrichment of the SCLM in trace elements after continental crust extraction (Hawkesworth et al., 1984). Some authors (Porcelli et al., 1986; Reid and Graham, 1996; Matsumoto et al., 2000; Dunaï and Porcelli, 2002) have introduced the

notion of rare gas mobility in the SCLM by infiltration of rare gas-bearing fluids from the asthenosphere.

Here, two possibilities arise, according to the way data are considered: the worldwide $^3\text{He}/^4\text{He}$ ratio can be viewed as either ranging between the MORB value and the more radiogenic one, without any preferential repartition (Dunai and Porcelli, 2002), or being centered around a constant, more radiogenic value than MORB (Gautheron and Moreira, 2002). In the former case, the infiltration of rare gases by metasomatism into the lithosphere should have occurred recently at preferential locations such as active rifting and/or volcanic areas, as enounced by Dunai and Porcelli (2002); thus, only a limited range of mixing between MORB and radiogenic helium would take place. In the latter case, the entire lithospheric mantle must be affected by a continuous metasomatism, which was modeled by Gautheron and Moreira (2002) as lithospheric helium being in steady-state relative to flux and radioactive production; helium residence time in the lithosphere and helium flux can then be calculated (see Gautheron and Moreira, 2002 for more details). In both cases, helium from the asthenosphere was added to the lithosphere, and radiogenic helium added to it. Both models have advantages and drawbacks, which are discussed in the following.

In the local, recent metasomatism model, MORB-like helium was introduced recently, at particular places into the lithosphere, where volcanism eventually occurs. During residence in the lithosphere, radiogenic helium is generated. According to the amounts of He and U introduced, and time when the

metasomatic event occurred, a range of $^3\text{He}/^4\text{He}$ ratios can be generated from MORB-like down to the lowest xenolith helium. This model would account for the range of $^3\text{He}/^4\text{He}$ ratios and calls for a relatively heterogeneous lithospheric helium.

The other possibility envisions that MORB-like helium, carried by metasomatic fluids and/or melts, continuously circulates upward across the entire lithosphere, where it becomes progressively more radiogenic due to U–Th radioactivity. The lithosphere would then be in steady-state for helium, and characterized by a relatively uniform value of the $^3\text{He}/^4\text{He}$ ratio because it has relatively constant U+Th concentration and also relatively constant thickness, hence helium residence time. We remark that, in this model, the lithosphere needs not to be a mixed reservoir; metasomatism only has to have a uniformly distributed spatial repartition.

Because the helium isotopic ratio of the European xenoliths is similar to the worldwide value (Gautheron and Moreira, 2002), the steady-state model can be applied to Europe with similar results: residence time ~15–150 Ma and a ^4He flux of 4.1×10^9 at/m²/s or a ^3He flux of 3.5×10^4 at/m²/s. Table 5 shows values of the ^4He flux obtained from He measurement for different areas in the world: lakes and volcanic provinces. The helium flux varies with type of sampling and location, showing that the transport of rare gases in the crust has preferential paths, as shown by Weinlich et al. (1999). The flux calculated by the steady-state model represents global continental degassing. The values measured in lakes, volcanic

Table 5
Examples of helium isotopic flux for lakes and volcanic provinces

Locality	Surface (km ²)	R/Ra	Flux ^4He (at/m ² /s)	Reference
Lake				
Laacher See (Germany)	3.31	5.36±0.02	(10±2)×10 ¹²	(Aeschbach-Hertig et al., 1996)
Lac Pavin (France)	0.44	6.57±0.01	(6±2)×10 ¹¹	(Aeschbach-Hertig et al., 1999)
Lake Nemrut (Turkey)	20	8.67	(2–3)×10 ¹¹	(Kipfer et al., 1994)
Lake Mashu (Japan)	20	6.81±0.12	9.2×10 ¹¹	(Igarashi et al., 1992)
Lake Nyos (Cameroon)	1.49	5.64	(3±0.4)×10 ¹⁴	(Sano et al., 1990)
Volcanic province				
Western Eger rift (Central Europe)	1500	5	1.2×10 ¹⁰	(Weinlich et al., 1999)
Great Hungary basin	50,000		9.2×10 ⁹	(Martel et al., 1989)*
Great Hungary basin	50,000		4.2×10 ⁸	(Stute et al., 1992)
This study	700,000	6.32±0.35	4.1×10 ⁹	

One ^4He flux (*) is calculated assuming a $^4\text{He}/^3\text{He}$ for the SCLM of 115,000 (R/Ra of 6.32) and that the difference with the asthenosphere is due to secondary ^4He radiogenic production.

provinces or sedimentary basins cannot be compared directly to the calculated flux because the lithosphere may have been degassed due to past volcanic activity. Nevertheless, calculated and measured fluxes are relatively close to each other, (Table 5) showing that the steady state model is consistent with the data and can account for the mantle helium flux in non-volcanic areas.

Global percolation through the entire SCLM is perhaps difficult to envision. Nevertheless, the similarity of the calculated helium flux to measured values for volcanic and basin areas, together with the homogeneous helium isotopic ratio observed for the European subcontinental lithosphere are arguments in favor of the steady state model (i.e. global percolation). However, the volcanism and rift areas certainly offer preferential channels where metasomatic fluids and/or melts can percolate, consistent with the local, recent metasomatism model. In conclusion, both models are possible and open to discussion.

5.2. Origin of the atmospheric component: source feature or air contamination?

Neon and argon isotopic ratios measured in samples from the three volcanic provinces indicate mixing between a MORB-like mantle component and an air-like component (Figs. 3–5). The latter can reflect a source signature or shallow level contamination.

5.2.1. Atmospheric rare gases in the subcontinental lithosphere?

The atmospheric signature can proceed from the dehydration of a subducted plate, where the rare gases are mostly removed from the plate and may be stored in the mantle wedge (i.e. the subcontinental mantle). These fluids are related to the U-rich fluids that change the activity ratios of U and Th in the mantle near subduction zones (Bourdon et al., 2003). Matsumoto et al. (2001) and Yamamoto et al. (2004) have shown evidence for the presence of recycled atmospheric rare gases derived from subducting slabs and preserved in the mantle, in Japanese peridotites and Siberian xenoliths, respectively. Assuming that part of the atmospheric rare gases survive in these mantle rocks, the atmospheric signature of the European xenoliths could be explained by such a deep atmospheric component.

5.2.2. Contamination of xenoliths at shallow depth

Another possibility to explain the neon and argon atmospheric component is shallow contamination introduced by percolation of basaltic melts or volatiles in the xenoliths or by contamination at the surface. Neon and argon data from worldwide xenoliths also show an atmospheric component. In several cases, the subcontinental lithosphere has not undergone a subduction stage (Marty et al., 1994; Matsumoto et al., 1998, 2000; Barfod et al., 1999). This may be an argument in favor of superficial atmospheric contamination of the xenoliths rather than the presence of a deep atmospheric component.

Sample DWC1 (Eifel, Germany) with the highest proportion of mantle neon was replicated by crushing, step crushing and after leaching with HF (Fig. 5). In the $^{40}\text{Ar}/^{36}\text{Ar}$ – $^3\text{He}/^{36}\text{Ar}$ diagram of Fig. 5, the straight line is due to mixing between a mantle component and air. The results for DWC1 c1 and c2 show that the atmospheric component is released during the first crushing step and the leached sample shows a more pristine signature than the un-leached samples. This experiment suggests that the European samples contain a large proportion of atmospheric contamination, and that leaching can remove a part of the atmospheric component. Additionally, the study of inclusions indicates the presence of CO_2 -rich fluid inclusions characterized by an homogenization temperature of 25 °C, that were thus generated at <20 km depth. The presence of this kind of inclusions can be due to percolation of fluids into the xenoliths at this depth, or to decrepitation and formation of secondary inclusions. The fact that the more abundant the CO_2 -rich inclusions, the more important the air-like component is consistent with the hypothesis of percolation of air-rich fluids into the xenoliths. This conclusion is in accordance with Andersen et al. (1984), who argue for infiltration into the xenoliths of basaltic melt and volatiles from the host basalts of Dreiser Weiher. Besides, Farley and Craig (1994) and Burnard et al. (1994) have reached the conclusion that an air component is present in phenocrysts, attributed to air assimilation (certainly by fracture annealing and/or bubble enclosure). Based on these conclusions, the atmospheric component in the xenoliths of this study can be explained by air-addition coming from the host magma. Additionally,

in the European samples, no correlation between observed ^3He and ^{36}Ar concentrations is observable indicating that we cannot argue for a dominant recycling origin of the air-like component in our samples (Matsumoto et al., 2001).

In the following, we will assume that the samples are air-contaminated and we will use the neon isotopes to constrain this contamination.

5.3. Elemental $^3\text{He}/^{36}\text{Ar}$ fractionation in mantle xenoliths

He and Ar data for mantle xenoliths of this study and from worldwide locations and geochemical context (Poreda and Farley, 1992; Dunai and Baur, 1995; Matsumoto et al., 1998, 2000) are characterized by a $^3\text{He}/^{36}\text{Ar}$ ratio distinctly lower than the MORB mantle source. Fig. 5B shows that the $^3\text{He}/^{36}\text{Ar}$ ratio for sample DWC1 extrapolated to a $^{40}\text{Ar}/^{36}\text{Ar}$ ratio of 44,000 is 0.11, while the MORB mantle source $^3\text{He}/^{36}\text{Ar}$ estimate is 0.7 (see Moreira et al., 1998). In this diagram, the other samples define straight lines with various slopes (not shown), indicating that variable $^3\text{He}/^{36}\text{Ar}$ fractionation occurred, independent of, and before mixing with air. These observations point to the presence in the lithospheric mantle of fluid inclusions with different $^3\text{He}/^{36}\text{Ar}$ ratios, which can be due to preferential loss of helium from the inclusions to the matrix of the mineral grains.

As we know that, in xenoliths, the rare gases mostly reside in fluid inclusions, it is not unreasonable to envision that helium could migrate from the fluid inclusions to the matrix of the minerals, especially if metasomatic fluids/melts percolate through the lithosphere. This migration was shown by Trull and Kurz (1993) to account for slow helium apparent diffusion rates measured for natural olivine and pyroxenes, while these authors attributed the high diffusion rates derived for the matrix to the presence of abundant defects and fractures. This approach may provide some insight into the mechanism of helium migration through the lithosphere (neon would probably be much slower, and argon would not move in such a way). Helium would possibly get more easily out of crystal matrix to circulating fluids/melts than out of fluid inclusions, thus leaving variably fractionated (decreased)

$^3\text{He}/^{36}\text{Ar}$ ratios as a geochemical trace in the fluid inclusions.

5.4. Ne and Ar isotopic compositions of the SCLM

The European subcontinental mantle shows radiogenic helium ratios compared to the MORB value. It is possible to calculate the amount of ^{21}Ne created by nucleogenic production associated with this radiogenic helium, as well as of radiogenic ^{40}Ar .

5.4.1. Subcontinental lithospheric neon

The production ratio $(^{21}\text{Ne}/^4\text{He})^*$ is constant in the mantle at 4.5×10^{-8} (Yatsevich and Honda, 1997; Leya and Wieler, 1999). Assuming initial neon ratios similar to the MORB mantle source (e.g. solar $^{20}\text{Ne}/^{22}\text{Ne}$ and $^{21}\text{Ne}/^{22}\text{Ne}=0.075$) one can write the following equation, assuming a constant $^3\text{He}/^{22}\text{Ne}$ ratio for the rare gases in the subcontinental lithospheric mantle:

$$\frac{^{21}\text{Ne}}{^{22}\text{Ne}} = \left(\frac{^{21}\text{Ne}}{^{22}\text{Ne}} \right)_{\text{MORB}} + \left(\frac{^{21}\text{Ne}}{^4\text{He}} \right)^* \times \left(\frac{^4\text{Ne}^*}{^3\text{He}} \right) \left(\frac{^3\text{He}}{^{22}\text{Ne}} \right) \quad (1)$$

We derive that the European lithospheric mantle has a $^{21}\text{Ne}/^{22}\text{Ne}$ end-member of 0.083 (with $^4\text{He}^*/^3\text{He}=115,000-90,000=25,000$ and $^3\text{He}/^{22}\text{Ne}=7$ (Moreira et al., 1998)). The $^3\text{He}/^{22}\text{Ne}$ ratio is assumed here to be similar in the SCLM and in the MORB source. This calculation shows that the hypothesis of SCLM-air mixing is coherent with a closed system He–Ne isotopic evolution. The mixing line with air (called here as “SCLM line”) corresponding to this value is shown in Fig. 3. One can observe that the data plot on this line even if the precision does not allow discriminating with certainty between the MORB line and this “SCLM line”. However, in our calculation, we assumed a $^3\text{He}/^{22}\text{Ne}$ of 7 for the SCLM, three times higher than the estimate of Ballentine (1997). Using the Ballentine’s value, we get a $^{21}\text{Ne}/^{22}\text{Ne}$ ratio very close to the MORB value (=0.077). Our data cannot discriminate between the two possibilities. Our samples suggest a $^3\text{He}/^{22}\text{Ne}$ ratio extrapolated to solar $^{20}\text{Ne}/^{22}\text{Ne}$ of 2 in agreement with Ballentine (1997).

5.4.2. Subcontinental lithospheric argon

Similarly to neon, the argon isotopic signature of the subcontinental lithospheric mantle can be derived from the following equation:

$$\frac{^{40}\text{Ar}}{^{36}\text{Ar}} = \left(\frac{^{40}\text{Ar}}{^{36}\text{Ar}} \right)_{\text{MORB}} + \left(\frac{^{40}\text{Ar}}{^4\text{He}} \right)^* \times \left(\frac{^4\text{He}^*}{^3\text{He}} \right) \left(\frac{^3\text{He}}{^{36}\text{Ar}} \right) \quad (2)$$

With $^{40}\text{Ar}/^{36}\text{Ar}_{\text{MORB}}=44,000$ (Moreira et al., 1998) (corresponding to a solar $^{20}\text{Ne}/^{22}\text{Ne}$ ratio); $(^{40}\text{Ar}/^4\text{He})^*=0.25$ with $K/U=12,700$; $^4\text{He}^*/^3\text{He}=25,000$ and $^3\text{He}/^{36}\text{Ar}_{\text{mantle}}=0.7$ (Moreira et al., 1998), the $^{40}\text{Ar}/^{36}\text{Ar}$ ratio of the SCLM is estimated to be 48,375, slightly more radiogenic than the MORB source value but still compatible with the xenolith data. The large atmospheric signature of the xenoliths cannot permit to test this hypothesis. Again, we have taken a $^3\text{He}/^{36}\text{Ar}$ similar to the upper mantle, which is not demonstrated.

5.5. Is there a Ne and Ar flux into the SCLM?

One hypothesis that can explain the peculiar helium isotopic signature of the European SCLM mantle is the steady state model. An important question is then: can we explore a similar model for neon and argon?

Using the mantle elemental ratios $^3\text{He}/^{22}\text{Ne}$ and $^4\text{He}/^{36}\text{Ar}$ of respectively 7 and 0.7 (Moreira et al., 1998), Ne and Ar fluxes can be calculated, using the ^3He flux of 3.5×10^4 $\text{at}/\text{m}^2/\text{s}$. The fluxes of ^{22}Ne and ^{36}Ar are, respectively, 0.5×10^4 and 5×10^4 $\text{at}/\text{m}^2/\text{s}$.

Nevertheless, it would be important to better understand the transport phenomena of the rare gases in the SCLM. Two possibilities are diffusion or melt/fluids percolation (advection). Diffusion could occur through solids or at grain boundaries. If diffusion is responsible for the rare gas flux, due to the different diffusion coefficients of helium, neon and argon in the mantle, their flux through the SCLM should be different from the above values (e.g. the He/Ne, He/Ar, Ne/Ar ratios should be enhanced). However, diffusion appears much too slow (Gautheron and Moreira, 2002) to account for the helium flux (references quoted in Table 5). The second possibility is percolation of melts or fluids generated by less than

1% melting of the asthenosphere. Noble gases are very incompatible elements (Graham, 2002), thus there is probably no elemental fractionation on melting, even at low melting rates. Exsolution of the fluid phase should next fractionate the rare gases, but it is difficult to quantify such a fractionation due to the many unknowns involved. However, percolation is compatible with large noble gas fluxes through the SCLM, and we argue that the helium flux coming with these melts and fluids is at steady state. These various possibilities have been extensively discussed by Dunai and Porcelli (2002).

Another important point is the possible recycling of atmospheric rare gases in the SCLM from past subduction. During dehydration of the subducting plate, the atmospheric rare gases may be carried out by fluids that metasomatize the mantle wedge (Tatsumi and Kogiso, 1997). Because the ^3He contents of the atmosphere and in the subducted slab are low compared to the mantle, ^3He is probably not significantly recycled and subduction does not affect the ^3He flux. This is not the case for neon and argon (Matsumoto et al., 2001; Yamamoto et al., 2004). Our theoretical estimate of neon and argon fluxes, based on the helium flux and mantle-like elemental ratios, are therefore minimum values, but it is impossible to compare them with measured values, since large air contamination occurs in lakes and well gases.

6. Conclusions

The rare gas signatures measured in xenoliths from a very large zone in Europe give constraints on the history and evolution of the subcontinental lithospheric mantle. The helium isotopic ratio is very constant and radiogenic compared to the MORB mantle source: 115,000 compared to 90,000. To explain this homogeneous helium signature, two models are invoked. In the first one, recent and local metasomatism by fluid and/or melt occurs in volcanism and/or active rifting areas. In the second model, metasomatism occurs globally through the entire SCLM, where helium is in steady state, i.e. ^4He is generated in the lithosphere by radiogenic production from U and Th decay, whereas ^3He derives from the asthenosphere with a flux of 3.5×10^4 $\text{at}/\text{m}^2/\text{s}$. This flux represents a global lithospheric value, and is consistent with estimates for

large basin degassing. Neon and argon show mixing between a MORB-like and an atmospheric component. Elemental fractionation of He/Ar ratios suggests that helium may diffuse out of fluid inclusions into the matrix of crystals. The He–Ne–Ar results argue against a primitive plume source in the European lithospheric mantle. The atmospheric component probably derives mainly from contamination close to the surface rather than from circulation of subduction-related fluids carrying air rare gases in the subcontinental mantle. Using the ^4He excess, and assuming an elemental rare gas composition similar to the upper mantle, we derive the ^{21}Ne and ^{40}Ar excesses in the subcontinental mantle. Air subduction may add a supplementary flux to the SCLM and change elemental and isotopic rare gas signatures for Ne and Ar.

Acknowledgement

We wish to thank J. Curtice and M. Kurz for measurements at WHOI. T. Dunai is warmly acknowledged for donating Germany and Austria samples. We also indebted to K. Farley and P. Sarda for their critical remarks that greatly improved the manuscript. We thanked D. Porcelli and an anonymous reviewer for their reviews which have greatly improved the quality of the manuscript. [SG]

References

- Ackert, R.P., et al., 1999. Measurements of past ice sheet elevations in interior West Antarctica. *Science* 286, 276–280.
- Aeschbach-Hertig, W., Kipfer, R., Hofer, M., Imboden, D.M., Wieler, R., Signer, P., 1996. Quantification of gas fluxes from the subcontinental mantle: the example of Laacher See, a maar lake in Germany. *Geochim. Cosmochim. Acta* 60, 31–41.
- Aeschbach-Hertig, W., Hofer, M., Kipfer, R., Imboden, D.M., Wieler, R., 1999. Accumulation of mantle gases in a permanently stratified volcanic lake (Lac Pavin, France). *Geochim. Cosmochim. Acta* 63, 3357–3372.
- Allège, C.J., Moreira, M., Staudacher, T., 1995. $^4\text{He}/^3\text{He}$ dispersion and mantle convection. *Geophys. Res. Lett.* 22 (17), 2325–2328.
- Andersen, T., Neuman, E.-R., 2001. Fluid inclusions in mantle xenoliths. *Lithos* 55, 301–320.
- Andersen, T., O'Reilly, S.Y., Griffin, W.L., 1984. The trapped fluid phase in upper mantle xenoliths from Victoria, Australia: implications for mantle metasomatism. *Contrib. Mineral. Petrol.* 88, 72–85.
- Ballentine, C.J., 1997. Resolving the mantle He/Ne and crustal $^{21}\text{Ne}/^{22}\text{Ne}$ in well gases. *Earth Planet. Sci. Lett.* 152 (1–4), 233–250.
- Barfod, D.N., Ballentine, C.J., Halliday, A.N., Fitton, J.G., 1999. Noble gases in the Cameroon line and the He, Ne, and Ar isotopic composition of high μ (HIMU) mantle. *J. Geophys. Res.* 104, 29509–29527.
- Basu, S., Renne, P., DasGupta, D., Teichmann, F., Poreda, R., 1993. Early and late alkali igneous pulses and a high ^3He plume origin for the Deccan Flood Basalts. *Science* 261, 902–906.
- Bourdon, B., Turner, S., Dosseto, A., 2003. Dehydration and partial melting in subduction zone: constraints from U-disequilibria. *J. Geophys. Res.* 108, 1–19.
- Burnard, P.G., Stuart, F.M., Turner, G., Oskarsson, N., 1994. Air contamination of basaltic magmas; implications for high $^3\text{He}/^4\text{He}$ mantle Ar isotopic composition. *J. Geophys. Res.* 99 (9), 17709–17715.
- Chauvel, C., Jahn, B.-M., 1983. Nd–Sr isotope and REE geochemistry of alkali basalts from the Massif Central, France. *Geochim. Cosmochim. Acta* 48, 93–110.
- Dixon, E., Honda, M., McDougall, I., Campbell, I., Sigurdsson, I., 2000. Preservation of near-solar isotopic ratios in Icelandic basalts. *Earth Planet. Sci. Lett.* 180, 309–324.
- Dodson, A., Kennedy, M.B., DePaolo, D.J., 1997. Helium and neon isotopes in the Innaha Basalt, Columbia River Basalt Group: evidence for a Yellowstone plume source. *Earth Planet. Sci. Lett.* 150, 443–451.
- Dodson, A., DePaolo, D.J., Kennedy, B.M., 1998. Helium isotopes in lithospheric mantle: evidence from Tertiary basalts of the western USA. *Geochim. Cosmochim. Acta* 62, 3775–3787.
- Dunai, T.J., Baur, H., 1995. Helium, neon and argon systematics of the European subcontinental mantle: implications for its geochemical evolution. *Geochim. Cosmochim. Acta* 59, 2767–2783.
- Dunai, T.J., Porcelli, D., 2002. Storage and transport of noble gases in the subcontinental lithosphere. In: Porcelli, C.J.B.D., Wieler, R. (Eds.), *Noble Gases in Geochemistry and Cosmochemistry. Reviews in Mineralogy and Geochemistry*.
- Farley, K.A., Craig, H., 1994. Atmospheric argon contamination of ocean island basalt olivine phenocrysts. *Geochim. Cosmochim. Acta* 58, 2509–2517.
- Gautheron, C.E., Moreira, M., 2002. Helium signature of the subcontinental lithospheric mantle. *Earth Planet. Sci. Lett.* 199, 39–47.
- Goes, S., Spakman, W., Bijwaard, H., 1999. A lower mantle source for Central European Volcanism. *Science* 286, 1928–1931.
- Graham, D., 2002. Noble gas isotope geochemistry of mid-ocean ridge and ocean island basalts: characterisation of mantle source reservoirs. In: Porcelli, C.J.B.D., Wieler, R. (Eds.), *Noble Gases in Geochemistry and Cosmochemistry. Reviews in Mineralogy and Geochemistry*.
- Graham, D.W., Humphris, S.E., Jenkins, W.J., Kurz, M.D., 1992. Helium isotope geochemistry of some volcanic rocks from Saint Helena. *Earth Planet. Sci. Lett.* 110, 121–131.
- Hanyu, T., Kaneoka, I., 1997. The uniform and low $^3\text{He}/^4\text{He}$ ratios of HIMU basalts as evidence for their origin as recycled materials. *Nature* 390, 273–276.

- Hart, S.R., Hauri, E.H., Oschmann, L.A., Whitehead, J.A., 1992. Mantle plumes and entrainment: isotopic evidence. *Science* 256, 517–520.
- Hawkesworth, C.J., Rogers, N.W., van Calsteren, P.W.C., Menzies, M.A., 1984. Mantle enrichment processes. *Nature* 311, 331–335.
- Hiyagon, H., Ozima, M., Marty, B., Zashu, S., Sakai, H., 1992. Noble gases in submarine glasses from mid-oceanic ridges and Loihi seamount: constraints on the early history of the Earth. *Geochim. Cosmochim. Acta* 56, 1301–13016.
- Hoernle, K., Zhang, Y.-S., Graham, D., 1995. Seismic and geochemical evidence for large-scale mantle upwelling beneath the eastern Atlantic and western and central Europe. *Nature* 374, 34–39.
- Honda, M., McDougall, I., Patterson, D.B., Doulgeris, A., Clague, D., 1991. Possible solar noble-gas component in Hawaiian basalts. *Nature* 349, 149–151.
- Igarashi, G., et Ozima, M., Ishibashi, J., Gamo, T., Sakai, H., Nojiri, Y., Kawai, T., 1992. Mantle helium flux from the bottom of Lake Mashu, Japan. *Earth Planet. Sci. Lett.* 108, 11–18.
- Jurine, D., Jaupart, C., Brandeis, G., 2003. Penetration of mantle plumes through the lithosphere. AGU Fall meeting, Abst. 2457.
- Kempton, P.D., Harmon, R.S., Stosch, H.-G., Hoefs, J., Hawkesworth, C.J., 1988. Open-system O-isotope behavior and trace element enrichment in the sub-Eifel mantle. *Earth Planet. Sci. Lett.* 89, 273–287.
- Kipfer, R., Aeschbach-Hertig, W., Baur, H., Hofer, M., Imboden, D.M., Signer, P., 1994. Injection of mantle type helium into Lake Van (Turkey): a clue quantifying deep water renewal. *Earth Planet. Sci. Lett.* 125, 357–370.
- Kurz, M.D., 1986. Cosmogenic helium in a terrestrial igneous rock. *Nature* 320, 435–439.
- Kyser, T.K., Rison, W., 1982. Systematics of rare gas isotopes in basic lavas and ultramafic xenoliths. *J. Geophys. Res.* 87 (B7), 5611–5630.
- Leya, I., Wieler, R., 1999. Nucleogenic production of Ne isotopes in Earth's crust and upper mantle induced by alpha particles from the decay of U and Th. *J. Geophys. Res.* 104, 15439–15450.
- Leyreloup, A.D., 1992. La croute metamorphique du sud de la France (Massif Central, Languedoc)-Geologie de surface et des enclaves remontees par les volcans cenozoiques, PhD, Universite de Montpellier, Montpellier.
- Martel, D.J., Deak, J., Dövényi, P., Horvath, F., O'Nions, R.K., Oxburgh, E.R., et al., 1989. Leakage of helium from the Pannonian basin. *Nature* 342, 908–912.
- Marty, B., 1993. He, Ar, Sr, Nd and Pb isotopes in the volcanic rocks from Afar: evidence for a primitive mantle component and constraints on magmatic sources. *Geochem. J.* 27, 219–228.
- Marty, B., Trull, T., Lussiez, P., Basile, I., Tanguy, J.C., 1994. He, Ar, O, Sr and Nd isotope constraints on the origin and evolution of Mount Etna magmatism. *Earth Planet. Sci. Lett.* 126, 23–39.
- Matsumoto, T., Honda, M., McDougall, I., O'Reilly, S., 1998. Noble gases in anhydrous lherzolites from the Newer Volcanics, southeastern Australia: a MORB-like reservoir in the subcontinental mantle. *Geochim. Cosmochim. Acta* 62, 2521–2533.
- Matsumoto, T., Honda, M., McDougall, I., O'Reilly, S.Y., Norman, M., Yaxley, G., 2000. Noble gases in pyroxenites and metasomatised peridotites from the Newer Volcanics, south-eastern Australia: implications for mantle metasomatism. *Chem. Geol.* 168, 49–73.
- Matsumoto, T., Chen, Y., Matsuda, J.-I., 2001. Concomitant occurrence of primordial and recycled noble gases in the Earth's mantle. *Earth Planet. Sci. Lett.* 185, 35–47.
- Menzies, M., Rogers, N., Tindle, A., Hawkesworth, C., 1987. Metasomatic and enrichment Processes in lithospheric peridotites, an effect of Asthenosphere–Lithosphere interaction. In: Halkworth, M.A. (Ed.), *Mantle Metasomatism*. Academic Press, London, pp. 313–361.
- Moreira, M., Kunz, J., Allègre, C.J., 1998. Rare gas systematics in popping rock: isotopic and elemental compositions in the upper mantle. *Science* 279, 1178–1181.
- Moreira, M., Doucelance, R., Dupré, B., Kurz, M., Allègre, C.J., 1999. Helium and lead isotope geochemistry in the Azores archipelago. *Earth Planet. Sci. Lett.* 169, 189–205.
- Moreira, M., Breddam, K., Curtice, J., Kurz, M., 2001. Solar neon in the Icelandic mantle: evidence for an undegassed lower mantle. *Earth Planet. Sci. Lett.* 185, 15–23.
- Ozima, M., Podosek, F.A., 1983. *Noble Gas Geochemistry*. In: Cambridge University Press, New York. 367 pp.
- Porcelli, D.R., O'Nions, R.K., O'Reilly, S.Y., 1986. Helium and strontium isotopes in ultramafic xenoliths. *Chem. Geol.* 54, 237–249.
- Porcelli, D.R., Stone, J.O.H., O'Nions, R.K., 1987. Enhanced $^3\text{He}/^4\text{He}$ ratios and cosmogenic helium in ultramafic xenoliths. *Chem. Geol.* 64, 25–33.
- Porcelli, D.R., O'Nions, R.K., Galer, S.J.G., Cohen, A.S., Matthey, D.P., 1992. Isotopic relationships of volatile and lithophile trace elements in continental ultramafic xenoliths. *Contrib. Mineral. Petrol.* 110, 528–538.
- Poreda, R.J., Farley, K.A., 1992. Rare gases in Samoan xenoliths. *Earth Planet. Sci. Lett.* 113, 129–144.
- Reid, M.R., Graham, D.W., 1996. Resolving lithospheric and sub-lithospheric contributions to helium isotope variations in basalts from the southwestern US. *Earth Planet. Sci. Lett.* 144, 213–222.
- Rosenbaum, J.M., Wilson, M., 1997. Multiple enrichment of the Carpathian–Pannonian mantle: Pb–Sr–Nd isotopes and trace element constraints. *J. Geophys. Res.* 102, 14947–14961.
- Sano, Y., Kusakabe, M., Hirabayashi, J.-I., Nojiri, Y., Shinohara, H., Njine, T., et al., 1990. Helium and carbon fluxes in Lake Nyos, Cameroon: constraints on next gas burst. *Earth Planet. Sci. Lett.* 99, 303–314.
- Sarda, P., Staudacher, T., Allègre, C.J., 1988. Neon isotopes in submarine basalts. *Earth Planet. Sci. Lett.* 91, 73–88.
- Sarda, P., Moreira, M., Staudacher, T., Schilling, J.-G., Allègre, C.J., 2000. Rare gas systematics on the southernmost Mid-Atlantic Ridge: constraints on the lower mantle and the Dupal source. *J. Geophys. Res.* 105, 5973–5996.
- Seber, D., Barazangi, M., Ibenbrahim, A., Demnati, A., 1996. Geophysical evidence for lithospheric delamination beneath the Alboran Sea and Rif-Betic mountains. *Nature* 379, 785–790.

- Seck, H.A., Wedepohl, K.H., 1983. Mantle xenoliths in the Rhenish Massif and the Northern Hessian depression. *Plateau Uplift*, 343–349.
- Staudacher, T., Sarda, P., Allègre, C.J., 1990. Noble gas systematics of Réunion Island, Indian Ocean. *Chem. Geol.* 89, 1–17.
- Stosch, H.G., 1987. Constitution and evolution of subcontinental upper mantle and lower crust in areas of young volcanism: differences and similarities between the Eifel (F.R. Germany) and Tariat Depression (central Mongolia) as evidenced by peridotite and granulite xenoliths. *Fortschritte der Mineralogie*.
- Stosch, H.-G., Lugmair, G.W., 1986. Trace element and Sr and Nd isotope geochemistry of peridotite xenoliths from Eifel (West Germany) and their bearing on the evolution of subcontinental lithosphere. *Earth Planet. Sci. Lett.* 80, 281–298.
- Stosch, H.-G., Seck, H.A., 1980. Geochemistry and mineralogy of two spinel peridotite suites from Dreiser Weiher. *Geochim. Cosmochim. Acta* 44, 457–470.
- Stosch, H.G., Lugmair, G.W., Kovalenko, V.I., 1986. Spinel peridotite xenoliths from the Tariat Depression, Mongolia: II. Geochemistry and Nd and Sr isotopic composition and their implications for the evolution of the subcontinental lithosphere. *Geochim. Cosmochim. Acta* 50, 2601–2614.
- Stute, M., Sonntag, C., Deak, J., Schlosser, P., 1992. Helium in deep circulating groundwater in the Great Hungarian Plain: flow dynamics and crustal and mantle helium fluxes. *Geochim. Cosmochim. Acta* 56 (5), 2051–2067.
- Tatsumi, Y., Kogiso, T., 1997. Trace element transport during dehydration processes in the subducted crust: 2. Origin of chemical and physical characteristics in arc magmatism. *Earth Planet. Sci. Lett.* 148, 207–221.
- Trieloff, M., Kunz, J., Clague, D.A., Harrison, D., Allègre, C.J., 2000. The nature of pristine noble gases in mantle plume. *Science* 288, 1036–1038.
- Trull, T.W., Kurz, M.D., 1993. Experimental measurements of ^3He and ^4He mobility in olivine and clinopyroxene at magmatic temperatures. *Geochim. Cosmochim. Acta* 57, 1313–1324.
- Wedepohl, K.H., Baumann, A., 1999. Central European Cenozoic plume volcanism with OIB characteristics and indications of a lower mantle source. *Contrib. Mineral. Petrol.* 136, 225–239.
- Weinlich, F.H., Bräuer, K., Kämpf, H., Strauch, G., Tesar, J., Weise, S.M., 1999. An active subcontinental mantle volatile system in the western Eger rift, Central Europe: gas flux, isotopic (He, C and N) and compositional fingerprints. *Geochim. Cosmochim. Acta* 63, 3653–3671.
- Wilson, M., Downes, H., 1991. Tertiary-quaternary extension-related alkaline magmatism in western and central Europe. *J. Petrol.* 32, 811–849.
- Wörner, G., Zindler, A., Staudigel, H., Schmincke, H.-U., 1986. Sr, Nd and Pb isotope geochemistry of Tertiary and Quaternary alkaline volcanics from West Germany. *Earth Planet. Sci. Lett.* 79, 107–119.
- Yamamoto, J., Kaneoka, I., Nakai, S., Kagi, H., Prikhod'ko, V., Arai, S., 2004. Evidence for subduction-related components in the subcontinental mantle from low $^3\text{He}/^4\text{He}$ and $^{40}\text{Ar}/^{36}\text{Ar}$ ratio in mantle xenoliths from Far Eastern Russia. *Chem. Geol.* 207, 237–259.
- Yatsevich, I., Honda, M., 1997. Production of nucleogenic neon in the Earth from natural radioactive decay. *J. Geophys. Res.* 102, 10291–10298.